Physica Scripta

PAPER

Higher-order exceptional points using lossfree negative-index materials

RECEIVED
25 April 2023

REVISED
16 July 2023

ACCEPTED FOR PUBLICATION
3 August 2023

PUBLISHED
14 August 2023

Xin-Zhe Zhang[1], **Li-Ting Wu**[2], **Ru-Zhi Luo**[1] **and Jing Chen**[1,3]

[1] MOE Key Laboratory of Weak-Light Nonlinear Photonics and School of Physics, Nankai University, Tianjin 300071, People's Republic of China
[2] School of Information and Communication Engineering, Nanjing Institute of Technology, Nanjing 211167, People's Republic of China
[3] Collaborative Innovation Center of Extreme Optics, Shanxi University, Taiyuan, Shanxi 030006, People's Republic of China

E-mail: njltwu@hotmail.com **and** jchen4@nankai.edu.cn

Keywords: non-Hermitian optics, exceptional points, parity-time symmetry

Abstract

Negative-index materials (NIMs) support optical anti-parity-time (anti-$\mathcal{PT}$) symmetry even when they are lossless. Here we prove the feasibility in achieving higher-order exceptional points (EPs) in lossfree waveguide arrays by utilizing the anti-$\mathcal{PT}$ symmetry induced by NIM. Numerical simulation about a third-order EP fits well with the coupled-mode theory. A scheme of achieving fourth-order EPs is also discussed. This work highlights the great potential of NIM in overcoming the obstacles of ordinary non-Hermitian optics, and the possibilities of combining anti-$\mathcal{PT}$, $\mathcal{PT}$, and Hermitian couplings for various purposes.

1. Introduction

Exceptional points (EPs) refer to the singular degeneracies of non-Hermitian wave/quantum systems [1–7], where all the eigenvalues and the eigenvectors of the effective Hamiltonian coalesce simultaneously. Its novel topology enables interesting mode switching behaviors when circling around it [6–10]. Furthermore, the coalescent eigenfunction at EPs is very sensitive to tiny perturbation in the effective Hamiltonian, so high-sensitivity applications [11–14] can be envisioned. The high sensitivity is also associated with stopped-light effect and enhanced density of states, and can be utilized for other interesting purposes such as in realizing coherent absorbers and lasers [15–17].

Parity-time ($\mathcal{PT}$) symmetric systems [1–5], which are non-Hermitian, are the widely utilized ones in realizing EPs that separate the complex and real spectra regimes of the Hamiltonian. Considering a system supporting two coupled entities with distributed gain and loss, the $\mathcal{PT}$ symmetry requires for $(PT)^{-1}\mathcal{H}PT = \mathcal{H}$, where $\mathcal{H}$ is the Hamiltonian, $P = [0, 1; 1, 0]$ induces a spatial reflection and leads to a position exchange of the two entities, and T operator leads to a time-reversal operation (calculates the complex conjugates of all the elements in the Hamiltonian) and has the effect of turning gain into loss and vice versa [18]. Since the number of coalescing eigenvalues and the eigenvectors determines the order of EPs, such a kind of non-Hermitian systems only supports second-order EPs (EP2 for brief). Higher-order EPs, at which more than two eigenvalues and eigenstates coalesce, could provide more degrees of freedom for artificially designing the topology, increase the frequency splitting, and enhance the sensitivity further. Consequently, people have proposed many schemes in achieving higher-order EPs by increasing the number of subsystems in various platforms such as photonic crystals, microcavities, lattices, resonator networks and waveguides (WGs) [11, 12, 18–34]. However, among all the non-idealities in experiments [34], the strictly requirement of delicate balance among the spatially distributed gain and loss is the detrimental one, which dramatically hinders the transfer of higher-order EPs from a curious mathematical object to realistic applications of our daily life. Ways to access high-order EPs without resorting to gain and loss are thus desired. Such a target is, in principle, achievable because non-Hermitian physics covers many miscellaneous categories including but not limited to the $\mathcal{PT}$ symmetry. In addition, to achieve a non-Hermitian Hamiltonian, besides introducing imaginary components (gain and loss) to the diagonal elements we can also just set the off-diagonal elements unequal. The later route

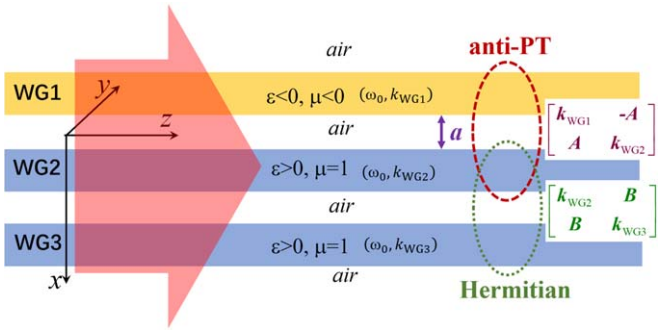

Figure 1. Schematic of the configuration under investigation, which contains three straight lossfree WGs. WG1 is made of a NIM with $\epsilon_{\rm NIM} = -3$ and $\mu_{\rm NIM} = -0.556$. WG2 and WG3 are made of dielectrics.

does not require gain and loss, and the whole energy can be conserved. A good example is the recently demonstrated anti-$\mathcal{PT}$ symmetry [$(PT)^{-1}\mathcal{H}PT = -\mathcal{H}$] associated with lossfree negative-index materials (NIMs) [35–40]. Due to the backward propagation of field in NIM, the coupling between a NIM WG and an ordinary dielectric WG can be modeled by an anti-$\mathcal{PT}$ Hamiltonian with unequal off-diagonal elements, and EP2s are shown to exist in the spectra of the guided waves [39, 40].

In this article, we prove the feasibility in realizing an optical third-order EP (EP3) by using the anti-$\mathcal{PT}$ symmetry induced by lossfree NIMs. A NIM-dielectric-dielectric WG configuration is utilized, which hybridizes the anti-$\mathcal{PT}$ symmetry of NIM-dielectric WG pair and Hermitian coupling of dielectric-dielectric WG pair together. Such a kind of configuration has not been discussed before, to the best of our knowledge. An effective non-Hermitian Hamiltonian is developed by using the coupled-mode theory (CMT) in order to explain the existence of EP3. This non-Hermitian Hamiltonian is different from other approaches of high-order EPs, because it is lossfree, and is neither $\mathcal{PT}$ symmetric nor anti-$\mathcal{PT}$ symmetric [11, 12, 18–34]. The transfer-matrix method (TMM) is utilized to numerically calculate eigensolutions of the guided modes, prove the existence of EP3, and reveal features of it. At the end of this article we also propose a scheme of realizing a fourth-order EP (EP4). This work proves that NIMs and the associated anti-$\mathcal{PT}$ symmetry have great potential in the study of non-Hermitian optics in lossfree environments for various applicable purposes.

This article is organized as follows. In section 2.1 we firstly propose the main concept of the coupled-WG structure and the physical mechanism of EP3 by using CMT. In section 2.2 we provide numerical calculation and analysis about the guided modes by using TMM. We show that the Hamiltonian from CMT can explain main features of the results from TMM, and prove the observed singular degeneracy is indeed an EP3. The analysis also provides more detailed information about how the eigenmodes evolve around EP3. Discussion about the importance of this study is provided in section 3. We also present a simple scheme of achieving an EP4 in section 3. Summary is made at the end of this article.

2. Theory and analysis

2.1. Structure, CMT and effective hamiltonian

Let us consider the structure shown in figure 1. It contains three straight WGs surrounded by air. All the media in this structure are lossfree. The lower two WGs (WG2 and WG3) are made of dielectrics with $\epsilon > 0$ and $\mu = 1$. The top WG1 is made of a NIM with $\epsilon_{\rm NIM} < 0$ and $\mu_{\rm NIM} < 0$. Because NIM requires an intrinsic dispersion of $\partial(\epsilon_{\rm NIM}\omega)/\partial\omega > 0$ and $\partial(\mu_{\rm NIM}\omega)/\partial\omega > 0$ so as to give a positive energy density [35–37, 40], in this article we would keep the angular frequency ω_0 a constant, and test the variation of the wavevectors β of the eigenmodes versus a geometric parameter of the structure.

Properties of the guided modes inside this structure can be found by using Maxwell's equations, see [15, 38–40]. As discussed in [39, 40], because the total energy should be conserved in this loss-free system, and the propagating directions of energy in the NIM and dielectric WGs are opposite to each other, the coupling between the top NIM WG1 and the adjacent dielectric WG2 is anti-$\mathcal{PT}$ symmetric [39, 40]. As for WG2 and WG3, their interaction can be described by using a Hermitian matrix. Only keeping the nearest-neighbor interaction, according to CMT the hybridization of the anti-$\mathcal{PT}$ symmetric interaction and the Hermitian one can be modeled by an effective Hamiltonian $\mathcal{H}$ in the form of

$$\begin{bmatrix} k_{\mathrm{WG1}} & -A & 0 \\ A & k_{\mathrm{WG2}} & B \\ 0 & B & k_{\mathrm{WG3}} \end{bmatrix} \begin{bmatrix} \psi_1 \\ \psi_2 \\ \psi_3 \end{bmatrix} = \beta \begin{bmatrix} \psi_1 \\ \psi_2 \\ \psi_3 \end{bmatrix}, \tag{1}$$

where β is the wavevector of the eigenmode, k_{WGi} is the resonant wavevector of mode in separate WGi ($i = 1, 2, 3$), and ψ_i represents an associated field component of it. Parameter A represents the strength of the anti-$\mathcal{PT}$ coupling between WG1 and WG2, and B is the Hermitian coupling strength between WG2 and WG3. Both A and B are real. Note that although this effective Hamiltonian $\mathcal{H}$ is non-Hermitian, it is neither $\mathcal{PT}$ symmetric nor anti-$\mathcal{PT}$ symmetric because $(PT)^{-1}\mathcal{H}PT$, where $P = [0, 0, 1; 0, 1, 0; 1, 0, 0]$, in general does not return $\mathcal{H}$ or $-\mathcal{H}$. Equation (1) generally has three solutions. Here let us assume the resonances in WG2 and WG3 are degenerated but different from that of WG1,

$$\begin{aligned} k_{\mathrm{WG1}} &= k_0 + 3\delta, \\ k_{\mathrm{WG2}} &= k_{\mathrm{WG3}} = k_0, \end{aligned} \tag{2}$$

where the factor 3 before δ is intentionally introduced in order to make below analysis concise. Substituting them into equation (1) and assume

$$y = \beta - k_0 - \delta, \tag{3}$$

the three solutions of β can be found by solving the secular equation

$$y^3 + C_1 y + C_0 = 0, \tag{4}$$

where the coefficients are given by

$$\begin{aligned} C_1 &= A^2 - B^2 - 3\delta^2, \\ C_0 &= (A^2 + 2B^2 - 2\delta^2)\delta. \end{aligned} \tag{5}$$

Because A, B, k_0 and δ are all real, C_0 and C_1 are also real valued.

Assuming the three solutions are $y_{1,2,3}$, equation (4) has many interesting properties such as $y_1 + y_2 + y_3 = 0$ and $y_1 y_2 y_3 = -C_0$. A notable feature is that it can support an EP3 with three identical solutions of $y = 0$ when

$$C_1 = C_0 = 0. \tag{6}$$

equation (6) can be satisfied only when the conditions of

$$\begin{aligned} \delta &= 0, \\ A^2 &= B^2 \end{aligned} \tag{7}$$

are met simultaneously. These are the existence conditions of EP3, the main conclusion of this article.

Because parameters A and B are tunable by managing the distances between adjacent WGs, to gain a deep insight about the formation of EP3 and the variation of the associated eigenvectors, let us check how the eigensolutions vary around EP3. Substituting $k_{\mathrm{WG1}} = k_{\mathrm{WG2}} = k_{\mathrm{WG3}} = k_0$ into equation (1) we can get

$$(\beta - k_0)^3 + (\beta - k_0)(A^2 - B^2) = 0. \tag{8}$$

Assuming all the solutions are real, we can sort them in ascending order. The solution β_2 is between the other two and is given by

$$\beta_2 = k_0, \tag{9}$$

which is a constant and does not depend on the values of A and B. The other two solutions are given by

$$\beta_{1,3} = k_0 \mp \sqrt{B^2 - A^2}, \tag{10}$$

which are complex (real) in the region of broken (exact) phase when $B^2 < A^2$ ($B^2 > A^2$). As for the eigenvectors, from equation (1) we can find

$$\begin{aligned} \Psi_2 &= \frac{1}{\sqrt{A^2 + B^2}}[B,\ 0,\ -A]^T, \\ \Psi_{1,3} &= \frac{1}{\sqrt{2}\,B}[A,\ \mp\sqrt{B^2 - A^2},\ -B]^T, \end{aligned} \tag{11}$$

respectively.

Once the condition of $A^2 = B^2$ is satisfied, a coalescence takes place, where all the three eigensolutions coalesce together. This coalescent point is an EP3, and the eigensolution and eigenvector are given by

$$\begin{aligned} \beta_{\mathrm{EP3}} &= k_0, \\ \Psi_{\mathrm{EP3}} &= \frac{1}{\sqrt{2}}\left[1, 0, -\mathrm{sign}\left(\frac{A}{B}\right)\right]^T, \end{aligned} \tag{12}$$

respectively, where the function sign(x) returns 1 (-1) when $x > 0$ ($x < 0$).

If the two conditions of equation (6) are not satisfied simultaneously, e. g. when $\delta \neq 0$, we could not access EP3. Now the system at most supports an EP2. One solution of β is always real, and the other two solutions are determined by

$$\Delta = \left(\frac{C_0}{2}\right)^2 + \left(\frac{C_1}{3}\right)^3. \tag{13}$$

When $\Delta = 0$, the two solutions are identical and an EP2 is achieved. When moving from $\Delta = 0$, for example, by changing the distance between two adjacent WGs so as to modify A or B, the system would enter either the exact or the broken non-Hermitian phase. If $\Delta > 0$, two complex conjugate solutions are achieved, and the system is within the broken phase. If $\Delta < 0$, two real solutions with different values are found, and the system is within the exact phase. In the next section we would demonstrate this phenomenon.

2.2. TMM Simulation and Analysis

The theory proposed in the above subsection is based on the effective Hamiltonian from CMT. When studying the guided modes in coupled WGs we should still resort to some rigorously numerical methods based on Maxwell's equations. Here we use TMM to analyze the transverse-electrical modes in the structure. In each layer the field is expressed as $E_y = [E_+ \exp(jk_i x) + E_- \exp(-jk_i x)]\exp(-j\beta z)$, where $k_i^2 + \beta^2 = \epsilon_i \mu_i \omega_0^2/c^2$, c is the speed of light. The transmission/reflection properties of the structure are summarized by $[E_t,\ 0]^T = \boldsymbol{M}\,[E_0,\ E_r]^T$, where $\boldsymbol{M}$ is the transfer matrix, E_0, E_t and E_r are the incident, transmitted, and reflected fields. At the top and bottom air layers surrounding the WGs, fields are required to exponentially decay away ($\mathrm{Im}\{k_i\} \neq 0$) so that the out-going boundary condition can be met. Wave-guiding is satisfied by the self-sustained condition of $M_{22} = 0$ [41] so that E_r and E_t are nonzero even when no incidence is present ($E_0 = 0$). In the phase-broken region where β is complex, similar process can be utilized by scanning β in the two dimensional space spanned by $\mathrm{Re}\{\beta\}$ and $\mathrm{Im}\{\beta\}$. As for the associated distributions of fields, they are also calculated by using TMM when the eigensolutions are found. Note that TMM can be applied to the transverse-magnetic modes as well by replacing E_y by H_y.

The geometric and optical parameters of the structure are set as follows. The thicknesses of all WGs are 4 cm. The distance between WG2 and WG3 is set to be 6 cm so that B is a constant here. The distance a between WG1 and WG2, which determines the value of A, is variable in our study. NIM is assumed to be the documented one with $\epsilon_{\mathrm{NIM}} = 1 - \omega_e^2/\omega^2$ and $\mu_{\mathrm{NIM}} = 1 - F\omega^2/(\omega^2 - \omega_m^2)$, where $\omega_e = 2\pi \times 10$ GHz, $\omega_m = 2\pi \times 4$ GHz, and F=0.56 [36, 37]. At $\omega_0 = 2\pi \times 5$ GHz (a free-space wavelength of 6 cm) the dispersion gives $\epsilon_{\mathrm{NIM}} = -3$ and $\mu_{\mathrm{NIM}} = -0.556$. Figures 2(a) and (c) display the spectra of β versus a when WG2 and WG3 are made of the same dielectric of $\epsilon = 4.504$. In this case $k_{\mathrm{WG2}} = k_{\mathrm{WG3}} \neq k_{\mathrm{WG1}}$ so we could only get an EP2. From the curves we can see the lower branch β_1 is always real, but the upper two branches β_2 and β_3 coalesce together in forming an EP2 at $a = 7.09$ cm. When a is smaller than 7.09 cm, the imaginary parts of these two branches are no longer zero, and the non-Hermitian phase is broken.

In order to realize an EP3, we should finely tune the parameters of the structure. When ϵ of the two dielectric WGs are modified by only 0.015% to 4.504 650 83, the dispersion curves are modified sharply and an EP3 is achieved, see figures 2(b) and (d). Now the initial lower branch β_1 coalesces with the upper two branches $\beta_{2,3}$ at a single point $a_c = 6.69$ cm and forms an EP3. When a becomes smaller, two branches of β become complex. The middle branch is always real and is almost a constant respect to a. Note that due to the coalescence at EP3, it is impossible to find the exact one-to-one correspondence of the complex branches at $a < a_z$ to these at $a > a_c$, so here the branches in the region of broken phase are still labeled in ascending order of $\mathrm{Im}\{\beta\}$.

Above numerical calculations are based on TMM, which is rigorous. Before discussing characteristics of EP3 we should check how they fit with the results of CMT. To do it, we perform a best fitting about the dispersion curves by numerically solving equation (1). We first fit the curves shown in figures 2(b) and 2(d) because they are governed by $\delta = 0$ and require less fitting parameters. The value of k_0 is given by the numerical value of $\beta_2 = 1.325144\ \mathrm{cm}^{-1}$ obtained from TMM. As for A and B, following [40] we assume

$$A = B \exp\left(-\frac{a - a_c}{L_d}\right), \tag{14}$$

where $a_c = 6.69$ cm is the position of EP3, and L_d is the decay length. The best fitting then tells $B = 1.22 \times 10^{-3}$ cm^{-1} and $L_d = 1.3$ cm. From the red circles in figures 2(b) and 2(d) we can see CMT predicts most features of the dispersion curves from TMM. The only minor discrepancy is about $\mathrm{Re}\{\beta\}$ in the broken phase region, which might be fixed by considering spatial dispersion.

We then try to fit the results shown in figures 2(a) and (c). Since the only difference of them from figures 2(b) and (d) is that the resonances in WG2 and WG3 are perturbed by the same amount, we would maintain all the parameters about figures 2(b) and (d) unchanged, and only introduce a tiny perturbation to $k_{\mathrm{WG2,\ WG3}}$, that $k_{\mathrm{WG2}} = k_{\mathrm{WG3}} = k_0 + \Delta k$. A best fitting is achieved when $\Delta k = -1.8 \times 10^{-4}\ \mathrm{cm}^{-1}$, as shown by the red circles.

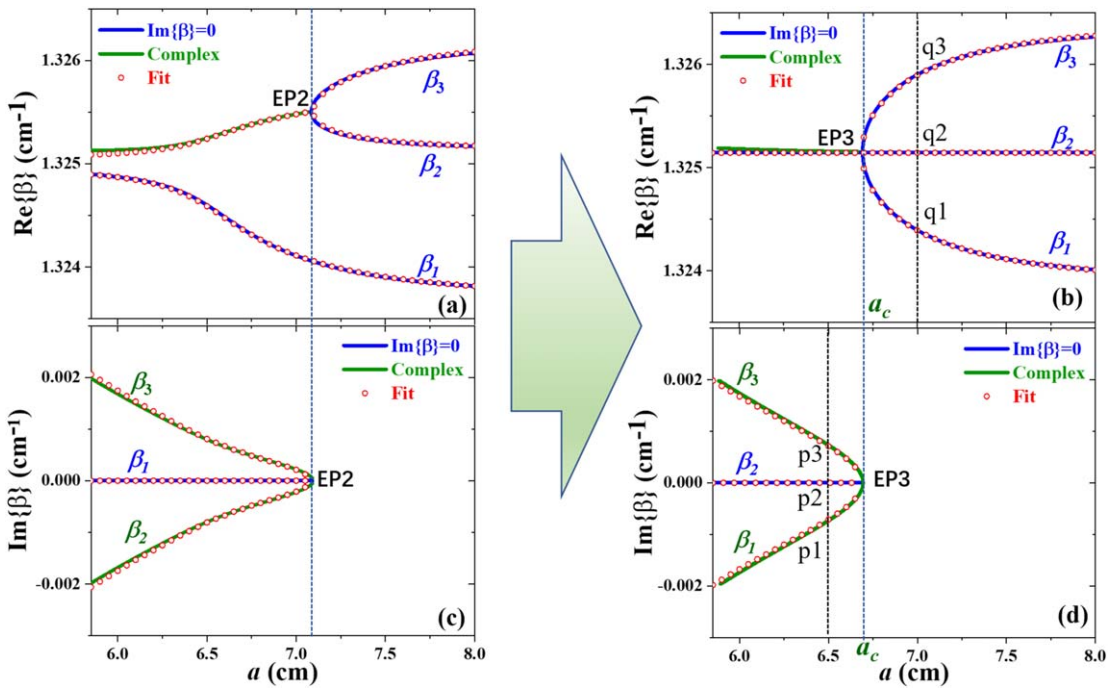

Figure 2. Variation of the eigensolutions β versus the distance a by using TMM. (a), (c) In general we can always get an EP2, where the other dispersion curve is real and always persists. (b), (d) By finely tuning parameters of the structure we can get an EP3. Red circles are the best fitted results by using equation (1). Im$\{\beta\}$ equals zero in the regions of exact phase and is not shown here.

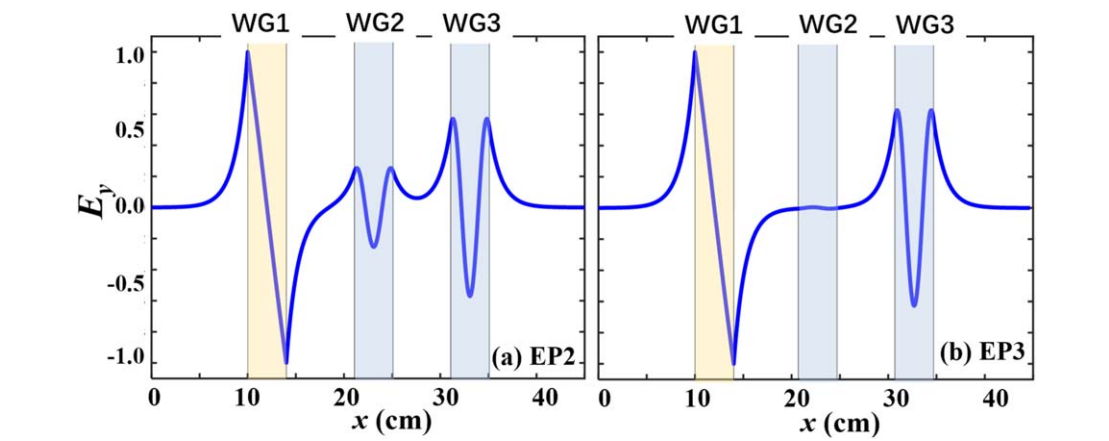

Figure 3. Distributions of fields E_y at (a) EP2 and (b) EP3 shown in figure 2. The fields are normalized by the maximum amplitudes in the structure.

We can see once again the results of CMT fits well with that from TMM. It confirms that CMT is an accurate model about the guided modes in the coupled WGs.

Now we can try to analyze the formation of EP3 and the associated characteristics of it. We first calculate the distributions of E_y at EP2 and EP3 of figure 2, and show them in figure 3. Note that because the values of β are real here and the whole structure is lossfree, the fields E_y inside the structure are made to be synchronous so that $\mathrm{Im}\{E_y\} = 0$. We can see EP3 is sharply different from EP2 because the field inside WG2 is nearly zero, which is in agreement with equation (12). The patterns of fields in WG1 (WG3) are similar with each other in the two scenarios.

We then pay attention to the structure supporting EP3, and calculate the distributions of E_y at six points around EP3 in the dispersion curves of figure 2(b) and (d). The results are shown in figure 4. A notable feature is that for the point $q2$ in the middle branch β_2, the field inside WG2 is very weak, similar to EP3. This phenomenon is also in agreement with equation (11) .

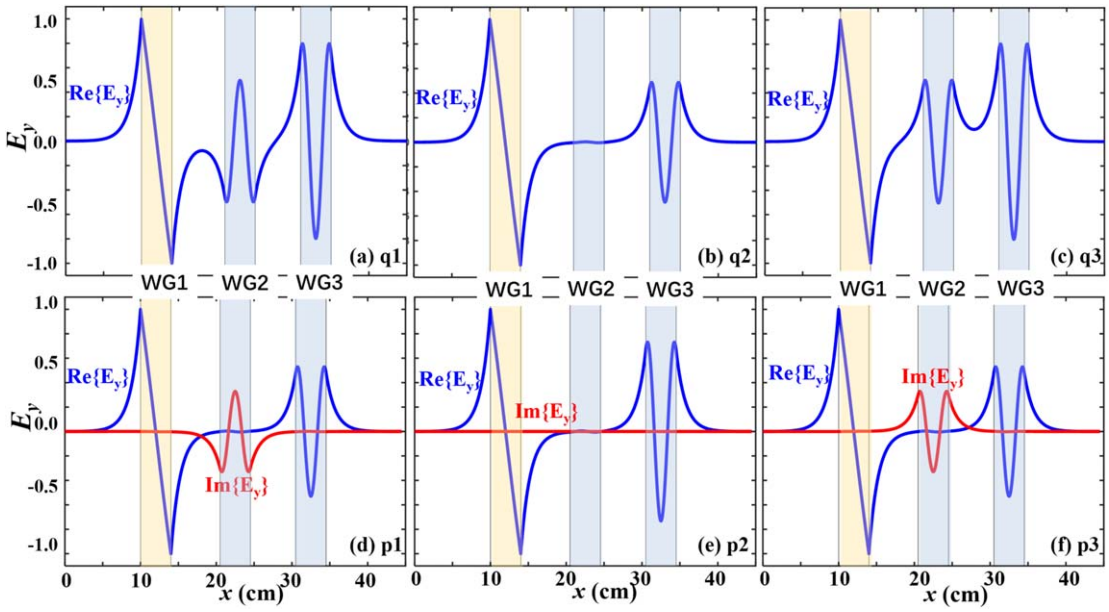

Figure 4. Distributions of fields E_y at the chosen points of figures 2(b) and (d) supporting EP3.

When $a < a_c$, two branches of β become complex. Now the fields E_y are no longer synchronous so in figures 4(d) to (f) we also plot the imaginary parts of E_y. From the distributions of fields we can see in the broken phase scenario, the patterns of ReE_y of the all three branches are almost identical with each other (also with that of EP3). The only differences in E_y are carried by the imaginary parts ImE_y. For the two complex-β branches, ImE_y are opposite to each other and are especially strong around WG2. This phenomenon can be explained by using equation (11), that in the region of broken phase, the complex amplitudes of the basic vector ψ_2 in $\Psi_{1,3}$ are purely complex and possess a $\pi/2$ phase difference from those of the basic vectors $\psi_{1,3}$.

To prove that at EP3 the three dispersion branches β indeed coalesce together, we test whether their eigenvectors follow the prediction of equation (11). It can be done by checking how the relative magnitude of field inside WG2 varies with a. Here we assume that ψ_i in the eigenvector represents E_y inside WGi ($i = 1, 2, 3$), calculate the integral of $|E|^2$ inside each WG, and find the ratio α of $|E|^2$ confined in WG2 by using

$$\alpha = \frac{\int_{\mathrm{WG2}} |E_y|^2 dx}{\int_{\mathrm{WG1}} |E_y|^2 dx + \int_{\mathrm{WG2}} |E_y|^2 dx + \int_{\mathrm{WG3}} |E_y|^2 dx}. \tag{15}$$

Albeit this approach is very rough because the fields outside WGs are ignored, the variation of α versus a shown in figure 5(a) agrees well with the dependence of $|\psi_2|^2$ on A given by equation (11). For modes in the middle branch β_2, α is nearly zero, which is in agreement with the null ψ_2 in Ψ_2. As for the other two branches, when a is much greater than a_c, the magnitude of A is much smaller than B, i.e. $|A| \ll |B|$. The eigenvectors are close to $[0, \pm 1, 1]^T$, and α approaches 50%. When a decreases so that A becomes comparable with B, α decreases sharply to zero. At a_c where $A = B$, as expected, a coalescence takes place. From this coalescence of α we can make the conclusion that this point at $a = a_c$ is not an accidental degeneracy of EP2 with other modes but a standard EP3.

Since EPs in $\mathcal{PT}$-symmetric WGs stop light [15, 16], we also calculate the group velocities v_g of the three branches. Here v_g is given by the ratio of the Poynting vector $S_z = -\int E_y H_x^* dx/2$ to the energy density $W = \int w dx$ via the formula $v_g = S_z/W$. When calculating the energy density we have adapted $w = \epsilon_0 \partial(\epsilon_{\mathrm{NIM}}\omega)/\partial\omega |E|^2/4 + \mu_0 \partial(\mu_{\mathrm{NIM}}\omega)/\partial\omega |H|^2/4$ in order to guarantee a positive energy. At 5GHz, the utilized dispersion of NIM gives $\partial(\epsilon_{\mathrm{NIM}}\omega)/\partial\omega = 5$ and $\partial(\mu_{\mathrm{NIM}}\omega)/\partial\omega = 4.975$. Figure 5(b) shows the variations of v_g versus a of the three branches β. When $a > a_c$ so that $A < B$, the β_2 branch possesses a negative group velocity. The reason is that for modes in this branch, over half of the field is localized in NIM WG1 supporting backward propagation of field. As for the other two branches, they are generally positive. When approaching a_c, all the branches coalesce together to v_g=0, which implies that at a_c the backward energy flux in the NIM WG1 balances the forward ones in WG1 and WG2, and in the surrounding air. This phenomenon is also demonstrated in [40] about EPs in NIM-dielectric WGs. Once again, figure 5(b) also provide an evidence that at a_c an EP3 is achieved.

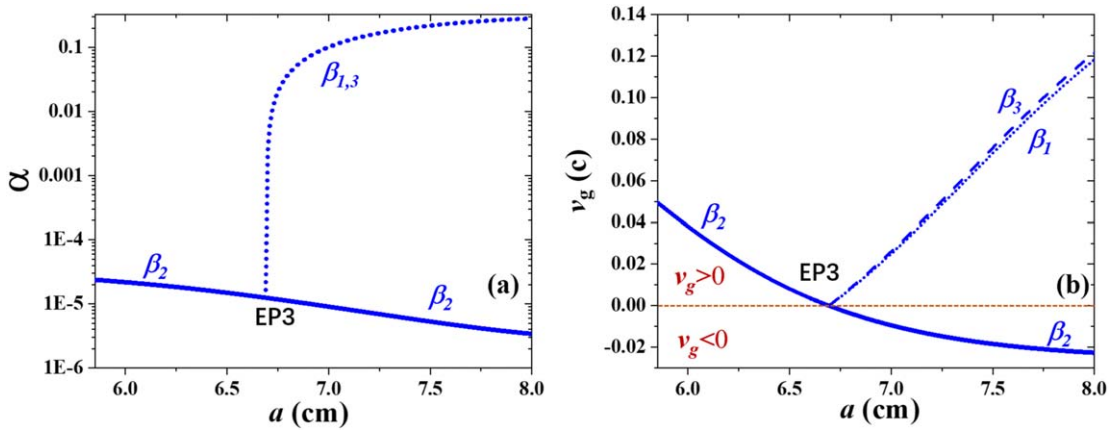

Figure 5. (a) Ratio of field localized inside WG2, where the y axis is plotted logarithmically. (b) Group velocities v_g of the three branches. Results about complex β are not shown because the associated α and v_g are not well defined.

3. Discussion

Up to now we have proved that it is feasible to achieve an EP3 in a lossfree WG system containing NIM. This kind of EP3 is produced via the hybridization of the anti-$\mathcal{PT}$ symmetric coupling in the NIM-dielectric pair and the Hermitian coupling in the dielectric-dielectric pair. No loss or gain is required. This work highlights the great potential of NIM in overcoming the obstacles of ordinary non-Hermitian optics, and the possibilities of combining anti-$\mathcal{PT}$, $\mathcal{PT}$, and Hermitian couplings for various purposes. Albeit in this article we only consider NIM-dielectric-dielectric configuration, EP3 can be achieved in the dielectric-NIM-NIM configuration as well because the coupling in the NIM-NIM pair is also Hermitian.

Our work provides a useful route to design lossfree systems in achieving EPs with higher orders by increasing the number of WGs [11, 12, 18–34]. For example, here we can propose a schematic structural design for an EP4 by using two dielectric and two NIM WGs. Arranging these four WGs parallel in the dielectric-dielectric-NIM-NIM order, and assuming their resonant wavevectors at ω_0 are k_1, k_2, k_1, and k_2, respectively, the effective Hamiltonian based on CMT with nearest-neighbor interaction can be expressed as

$$\begin{bmatrix} k_1 & A & 0 & 0 \\ A & k_2 & B & 0 \\ 0 & -B & k_1 & C \\ 0 & 0 & C & k_2 \end{bmatrix} \begin{bmatrix} \psi_1 \\ \psi_2 \\ \psi_3 \\ \psi_4 \end{bmatrix} = \beta \begin{bmatrix} \psi_1 \\ \psi_2 \\ \psi_3 \\ \psi_4 \end{bmatrix}, \tag{16}$$

where A, B, and C are all real for simplification. Assuming

$$k_{1,2} = k_0 \pm \delta, \tag{17}$$

it is then easy to prove that under the conditions of

$$\begin{aligned} B &= \pm(|A| + |C|), \\ \delta^2 &= |AC|, \end{aligned} \tag{18}$$

all the four eigensolutions coalesce together and form an EP4 at

$$\beta_{\mathrm{EP4}} = k_0. \tag{19}$$

The hierarchical construction of higher-order EPs by using above proposed method deserves a further discussion. Future attention could also be paid to the nonclassical nature of fields in this hybrid optical systems [42].

4. Conclusion

In summary, here we show it is feasible to achieve an EP3 in loss-free WGs by utilizing the anti-$\mathcal{PT}$ symmetry induced by NIM. We propose a configuration made of one NIM WG and two dielectric WGs, and suggest to hybridize the anti-$\mathcal{PT}$ symmetric interaction in the NIM-dielectric WG pair with the Hermitian interaction in the dielectric-dielectric WG pair together. Such a kind of configuration has not been discussed before, to the best of our knowledge. An effective lossfree non-Hermitian Hamiltonian is developed by using CMT, which is neither $\mathcal{PT}$ symmetric nor anti-$\mathcal{PT}$ symmetric. TMM simulation agrees well with the prediction of CMT, and

the features about EP3 in the coupled WG structure are discussed. A structure in supporting EP4 is also designed. This work highlights the great potential of NIM in overcoming the obstacles of ordinary non-Hermitian optics, and the possibilities of combining anti-$\mathcal{PT}$, $\mathcal{PT}$, and Hermitian couplings for various purposes.

Acknowledgments

This work was supported by the Natural National Science Foundation of China (NSFC) (12104227, 12 274 241), and the Scientific Research Foundation of Nanjing Institute of Technology (YKJ202021).

Data availability statement

All data that support the findings of this study are included within the article (and any supplementary files).

ORCID iDs

Jing Chen https://orcid.org/0000-0001-5637-1829

References

[1] Feng L, El-Ganainy R and Ge L 2017 *Nat. Photo.* **11** 75262
[2] El-Ganainy R, Makris K G, Khajavikhan M, Musslimani Z H, Rotter S and Christodoulides D N 2018 *Nat. Phys.* **14** 11
[3] Cao H and Wiersig J 2015 *Rev. Mod. Phys.* **87** 61
[4] Ozdemir S K, Rotter S, Nori F and Yang L 2019 *Nat. Mater.* **18** 783
[5] Miri M A and Alù A 2019 *Science* **363** eaar7709
[6] Khurgin J B, Sebbag Y, Edrei E, Zektzer R, Shastri K, Levy U and Monticone F 2021 *Optica* **8** 563
[7] Chen H Z *et al* 2020 *Nat. Phys.* **16** 571
[8] Shu X, Li A, Hu G, Wang J, Alu A and Chen L 2022 *Nat. Comm.* **13** 2123
[9] Nasari H, Lopez-Galmiche G, Lopez-Aviles H E, Schumer A, Hassan A U, Zhong Q, Rotter S, LiKamWa P, Christodoulides D N and Khajavikhan M 2022 *Nature* **605** 256
[10] Doppler J, Mailybaev A A, Bohm J, Kuhl U, Girschik A, Libisch F, Milburn T J, Rabl P, Moiseyev N and Rotter S 2016 *Nature* **537** 76
[11] Lin Z, Pick A, Loncar M and Rodriguez A W 2016 *Phys. Rev. Lett.* **117** 107402
[12] Hodaei H, Hassan A U, Wittek S, Garcia-Gracia H, El-Ganainy R, Christodoulides D N and Khajavikhan M 2017 *Nature* **548** 187
[13] Chen W, Ozdemir S K, Zhao G, Wiersig J and Yang L 2017 *Nature* **548** 192
[14] Wiersig J 2016 *Phys. Rev.* A **93** 033809
[15] Goldzak T, Mailybaev A A and Moiseyev N 2018 *Phys. Rev. Lett.* **120** 013901
[16] Zhang X Z, Luo R Z and Chen J 2022 *Opt. Express* **30** 38753
[17] Pick A, Zhen B, Miller O D, Hsu C W, Hernandez F, Rodriguez A W, Soljacic M and Johnson S G 2017 *Opt. Express* **25** 012325
[18] Li A *et al* 2023 *Nat. Nanotechnol.* **18** 706
[19] Jing H, Ozdemir S K, Lu H and Nori F 2017 *Sci. Rep.* **7** 3386
[20] Schnabel J, Cartarius H, Main J, Wunner G and Heiss W D 2019 *Phys. Rev.* A **95** 053868
[21] Pan L, Chen S and Cui X 2019 *Phys. Rev.* A **99** 011601
[22] Habler N and Scheuer J 2020 *Phys. Rev.* A **101** 043828
[23] Wang X, Guo G and Berakdar J 2021 *Phys. Rev. Appl.* **15** 034050
[24] Wu Y L, Zhou P J, Li T, Wan W S and Zou Y 2021 *Opt. Express* **29** 6080
[25] Xiong W, Li Z, Song Y, Chen J, Zhang G Q and Wang M 2021 *Phys. Rev.* A **104** 063508
[26] Novitsky A, Morozko F, Gao D, Gao L, Karabchevsky A and Novitsky D V 2022 *Phys. Rev.* B **106** 195410
[27] Zhong Q, Kou J, Ozdemir S K and El-Ganainy R 2020 *Phys. Rev. Lett.* **125** 203602
[28] Wiersig J 2022 *Phys. Rev.* A **106** 063526
[29] Benisty H, Lupu A and Degiron A 2015 *Phys. Rev.* A **91** 053825
[30] Heiss W D and Wunner G 2016 *J. Phys. A: Math. Theor.* **49** 495303
[31] Demange G and Graefe E M 2012 *J. Phys. A: Math. Theor.* **45** 025303
[32] Zhang S M, Zhang X Z, Jin L and Song Z 2020 *Phys. Rev.* A **101** 033820
[33] Zhang Y R, Zhang Z Z, Yuan J Q, Kang M and Chen J 2019 *Frontiers of Physics* **14** 53603
[34] He B, Yang L, Zhang Z and Xiao M 2015 *Phys. Rev.* A **91** 033830
[35] Veselago V G 1968 *Sov. Phys. Usp.* **10** 509
[36] Peacock A C and Broderick N G R 2003 *Opt. Express* **11** 2502
[37] Shadrivov I V, Sukhorukov A A and Kivshar Y S 2003 *Phys. Rev.* E **67** 057602
[38] Yariv A 1973 *IEEE J. Quantum Electron.* **9** 919
[39] Mealy T and Capolino F 2023 *Phys. Rev.* A **107** 012214
[40] Wu L T, Zhang X Z, Luo R Z and Chen J 2023 *Opt. Express* **31** 14109
[41] Longhi S 2010 *Phys. Rev.* A **82** 031801
[42] Agarwal G S and Qu K 2012 *Phys. Rev.* A **85** 031802(R)